Reverse Engineering of Materials using Image Processing Methods for CAD-Material Integration

David W. Rosen, Namin Jeong
The George W. Woodruff School of Mechanical Engineering
Georgia Institute of Technology
Atlanta, GA 30332-0405

Integration of material composition, microstructure, and mechanical properties with geometry information enables many product development activities, including design, analysis, and manufacturing. In this paper, we investigate the application of image processing methods for constructing models of material microstructure. These microstructure models can be integrated into CAD models to enable the utilization of material process-structure-property relationships during CAD modeling. Engineering design is enabled by integration of computational materials design methods with these relationships. Using 2D images and 3D voxel datasets, the image processing methods can be used to find microstructure features, such as grain boundaries or particle or fiber reinforcements, by finding edges and extracting features from those edges. This paper will focus on three different image processing methods, which will be applied to microstructure images of materials fabricated by additive manufacturing.

1 INTRODUCTION

For many years, practitioners in the additive manufacturing (AM) industry have complained about the lack of suitable engineering materials. Others note the large variability and unpredictability of mechanical properties in AM processed materials. Both sets of users would benefit from computer-aided design (CAD) tools that integrate material information with geometry. Furthermore, the capability of deriving mechanical properties from the material and geometry information would greatly aid part design and engineering. [1] In heterogeneous CAD modeling, models of both part geometry and material composition are integrated. In existing methods, material composition is typically specified parametrically using volume fractions where continuous distributions of material compositions are modeled. This approach is only appropriate for macro-scale part models, where detailed microscopic structures are not considered. Furthermore, such material composition models only represent the designer's desires or specifications, but the physical behavior of the actual materials is not recognized. Also, the actual material composition may deviate from the specification due to the specifics of manufacturing processes, heat treatments, or other material limitations. In this paper, we investigate the application of image processing methods for constructing models of material microstructure.

In recognition of the need of microscopic materials modeling for heterogeneous CAD systems, we present a new method for reverse engineering of composite materials such that models of material microstructure can be constructed and used as CAD representations to support heterogeneous part modeling. Such material models capture microscopic features and enable integration with structure-property relationships.

The proposed method for reverse engineering of materials is shown schematically in Figure 1. A material sample is sliced and imaged at appropriate resolutions to capture its microstructure and enable construction of process-structure-property relationships at the smallest size scale of interest. Before image analysis, the user specifies material compositions (i.e., which colors or shades correspond to which materials). Image processing method is applied to extract the geometry of the material's microstructure (e.g., grain or particle size, shape, orientation) and correlate it with material compositions. Next, models are constructed that enable properties of interest to be determined. For example, a material's elastic modulus and Poisson's ratio can be estimated from finite-element analysis. From the microstructure, process-structure relationships can also be determined. As a result, we will have the capability of constructing heterogeneous models of materials that can be integrated into CAD systems and used for mechanical part design.

In this paper, we will focus on the recognition of linear features of the material's microstructure using several image-processing methods. In the remainder of the paper, in section 2, a brief background review of image processing methods, surfacelet functions, edge detection method, and contour models, are introduced. In Section 3, feature extraction method from images based on the proposed image processing methods is described. Furthermore, the result of feature extraction and its discussion will be followed in section 4. Lastly, conclusion will be given in section 5.
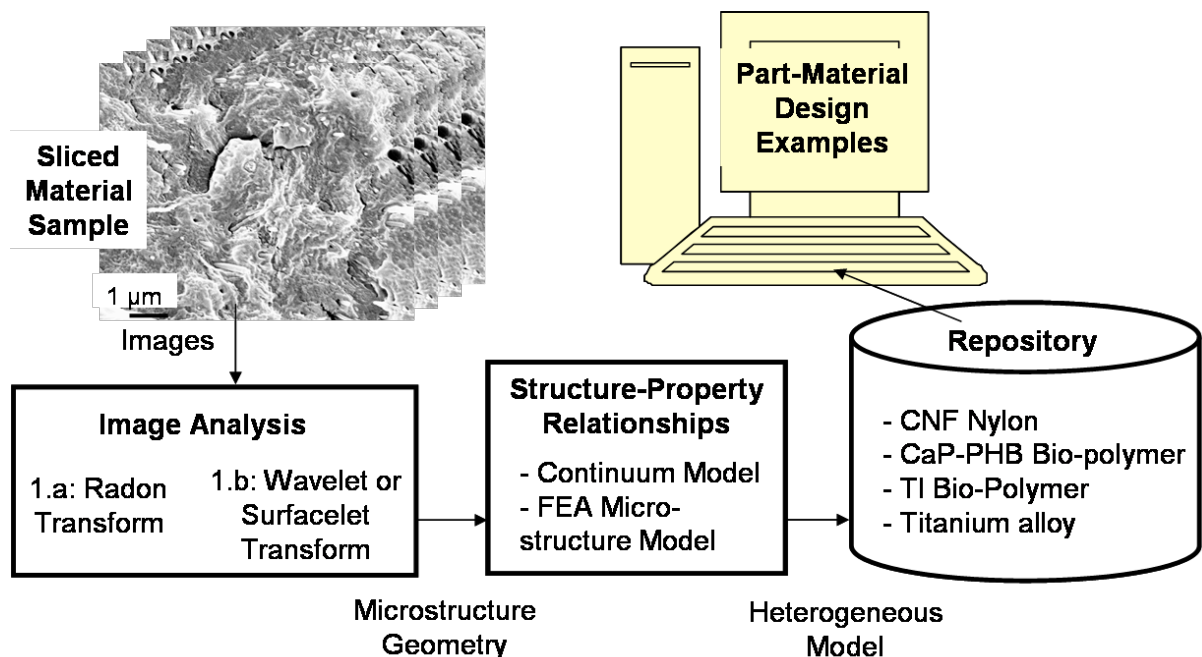
Figure 1 proposed reverse engineering of material process

2   BACKGROUND

Image processing converts an input image signal into either a different type of image or a set of characteristics of image [2]. This process enables a user to extract geometry features from an image. In microstructure images, geometric features are indicated by contours. In order to

recognize geometry entities, the contours must be detected and, preferably, be described by geometric entities such as line segments, circular arcs, or other analytic function. Of interest in this paper is linear microstructure features, including grain boundaries, fibers in fiber-reinforced polymer composites, and other features that appear as line segments. Since we are also interested in more general feature shapes, the image processing methods to be investigated in this paper will generalize to arbitrary feature shapes. Identified geometric features will be characterized by their position, orientation, and size. Automated feature extraction enables microstructure characterization that will aid greatly the development of material structure-property relationship databases.

Three general types of image processing methods will be investigated in this paper. First, the traditional edge detection method, the Canny method, is easy to use for extracting geometry characteristics in the image [3]. It uses the gradient of an image and typically produces a binary image as its output. Edges are not explicitly represented, but can be recognized using contour generation algorithms. The second type of method is a class of active contour models that seeks to fit curves to regions of the image with large gradients [4]. Energy minimization methods are typically used to ensure that the curves are smooth and they follow image contours closely. The third type of method is based on template matching methods that attempt to fit lines, line segments, or other shapes (templates) to regions of an image. The methods of interest here include Radon [5] and Hough transforms that use lines. Each method will be described in more detail in the next section.

3   FEATURE EXTRACTION METHOD
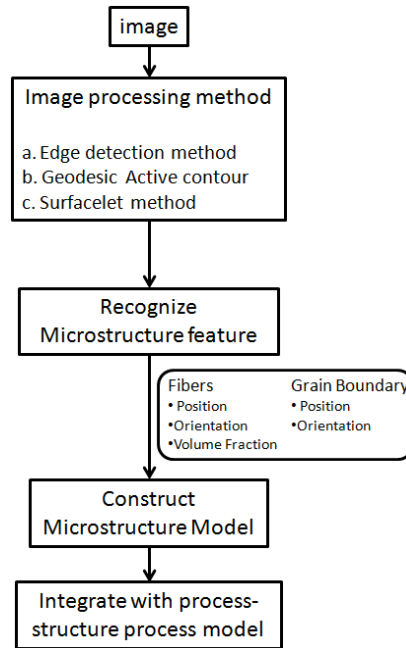
Figure 2 Process of reverse engineering with different image processing methods

In this section, we present the first step of the reverse engineering of materials procedure, from Figure 1. We use micro-scale images such as those from atomic force microscopy and electron microscopy to characterize a material's structure. As shown in Figure 2, various image processing methods are used to recognize microstructure features in the image. Image processing

methods extract geometry features from the image. Once geometry features are detected, the information is converted to a microstructure model. By integrating obtained information from the previous step, structure-property relationships can be achieved.

3.1 Edge detection method

In 1986, J. Canny investigated an edge detection operator, Canny edge detector, which uses a multi-stage algorithm to detect a wide range of edges in images [6]. His work focused on three requirements, good detection, good localization, and minimal response by finding the function which optimize a given functional. This edge detection method includes four stages, with some optional refinements possible. The first stage is noise reduction, which uses a filter based on a Gaussian, where the raw image is convolved with a Gaussian filter. This stage causes the input image to become slightly blurred, which reduces the affect of a minor amount of random noise. At the second stage of the algorithm, four filters are used to detect edges regardless of their orientation (horizontal, vertical, and diagonal). The third stage is non-maximum suppression, which estimates image gradients and performs a search to determine if the gradient magnitude assumes a local maximum in the gradient direction. Then, the method traces edges through the image and uses thresholding with hysteresis; that is, uses two threshold values, one for strong edges and one for weak edges. Since it is impossible to determine a generally applicable threshold for the method, the Canny method utilizes user defined thresholds. After finishing this stage, a binary image is produced where each pixel is marked as either an edge or a non-edge pixel. An optional differential geometry formulation for the third stage provides a more refined approach to obtain edges with sub-pixel accuracy.

The Canny algorithm plays powerful role in detecting edges. In addition, it is adaptable to various conditions to recognize the edges of differing characteristics depending on the particular requirements of a given implementation.

The result of Canny edge detection is a binary image, with edge pixels highlighted against a dark background. As such, the method does not accomplish microstructure feature extraction, since no higher level microstructure features are represented directly. However, the output images for Canny edge detection may be useful as inputs to more powerful methods, such as those to be presented.

3.2 Contour model

Kass et al. [7] focused on "snakes" or active contour models for boundary detection. The classical approach is based on deforming an initial contour towards the boundary of the object to be detected. The method minimizes an energy functional and therefore exhibits dynamic behavior [7]. If $C(q): [0,1] \rightarrow R^2$ is a parameterized planar curve and $I: [0,a] \times [0,b] \rightarrow R^+$ is a given image in which we want to detect the objects boundaries[8], then the general equation for active contour models can be expressed as

$$E(C) = \alpha \int_0^1 |C'(q)|^2 dq + \beta \int_0^1 |C''(q)|^2 dq - \lambda \int_0^1 |\nabla I(C(q))| dq \qquad (1)$$

where α, β, and λ are real positive constant. Eqn.1 consists of internal energy term and external energy term. Internal energy is

$$\alpha \int_0^1 |C'(q)|^2 dq + \beta \int_0^1 |C''(q)|^2 dq \qquad (2.a)$$

The first-order term makes the snake act like a membrane and the second-order term makes it act like a thin plate. Adjusting the weights α and β controls the relative importance of the membrane and thin-plate terms [7]. On the other hand, external energy is the rest of term of Eqn.1.

$$-\lambda \int_0^1 |\nabla I(C(q))| dq \qquad (2.b)$$

It consists of an image force and a constraint force [7]. Some drawbacks have been observed such that it can often be stuck in local minima state. In addition, this energy model is not capable of detecting an unknown number of objects simultaneously [8]. Therefore, special topology-handling procedures must be added. Regarding model accuracy, it is governed by the convergence criteria used in the energy minimization technique; higher accuracies require tighter convergence criteria and hence, longer computation times.

The geodesic active model is a particular case of the classical energy snake model that utilizes a level-set approach to identify contours in the image, guided by intrinsic geometric measures of the image [8]. Geodesic active contour is represented in the form of a zero set of a function. It is proved equivalent to finding a geodesic curve in a Riemannian space with a metric derived from the image content. Boundary detection can be considered equivalent to finding a curve of minimal weighted length in a certain framework [8]. The general equation is

$$E(C) = \alpha \int_0^1 |C'(q)|^2 dq - \lambda \int_0^1 |\nabla I(C(q))| dq \qquad (3)$$

The rigidity coefficient, β, from Eqns 1-2 is set equal to 0 in the geodesic active model. The regularization effect on the geodesic active contour comes from curvature based curve flows, obtained only from the other terms in Eqn.1. This will allow achieving smooth curves in the proposed approach without having the high order smoothness given by β≠0 in energy based approaches [8]. The most interesting feature of this geodesic active contour is that it allows automatic changes in the topology when implemented. Thereby, several objects can be detected simultaneously without previous knowledge of their exact number of in the scene and without using special tracking procedures. However, because this model only depends on the image gradient, to stop the curve evolution, the model can detect objects with edges defined by gradient [8].

In addition, geodesic active contour is developed to overcome the major drawbacks of the classical active contour model, which uses a local gradient-based edge detector to stop the evolving curve on object boundaries [9]. Table 1 shows the process of finding grain boundaries using both the classical active contour and the geodesic active contour models. The active contour model uses seeds provided manually by the user and only detects one grain boundary at one time, while the geodesic active contour model detects all grain boundaries at the same time. Our implementation of the geodesic active contour model provides equally spaced seeds and allows the user to adjust their size, number, and location. The seed evolves by itself, searching minimum weighted length. When it finds a minimum value, the seed stops its expansion.

Table 1 Result of curve evolving in both active contour model and geodesic active contour

Active contour model	Geodesic active contour
a. Initial stage	b. Initial stage
c. Middle stage	d. Middle stage
e. Final stage	f. Final stage
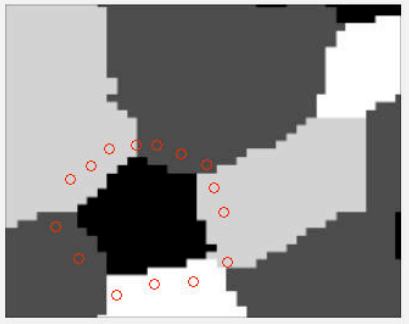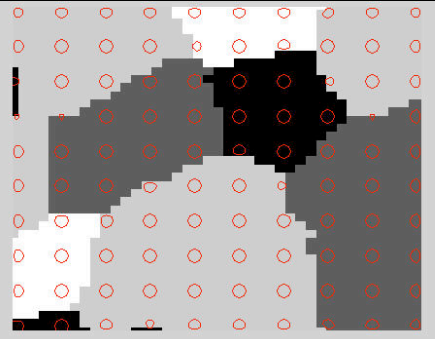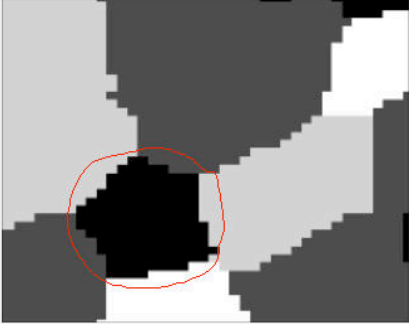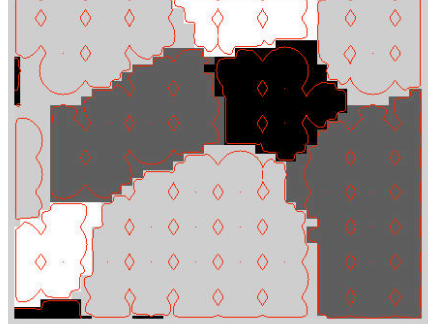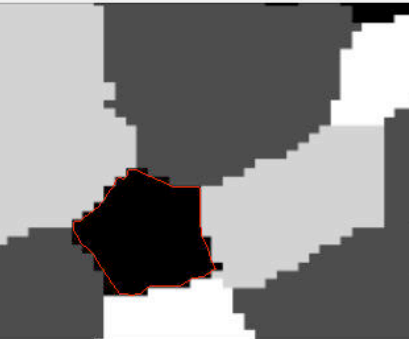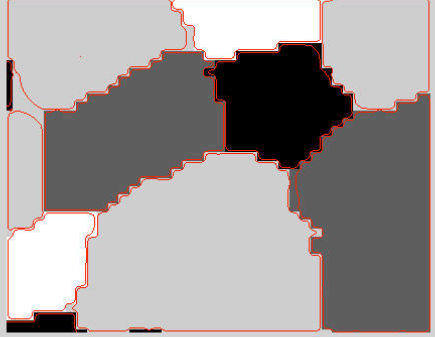
3.3 Surfacelet method

As introduced in [5], surfacelet models can be generated by a combination of Radon-like surfacelet and wavelet transforms. In this paper, we only consider the Radon transform, a special case of surfacelet transform, in the analysis.

The Radon transform is an effective method for representing line singularities in images [5]. The Radon transform was developed to reconstruct images from CT scans [10], which consist of sets of parallel scans where the source and sensor rotate around the target. We use Radon transform to fit surfacelet models to microstructures. Then, by applying a wavelet transform to the results of the Radon transform, an image representation is produced. Mathematically, the Radon transform in a domain Ω is the integral along the plane (represented as the dash line in 2D),

which is perpendicular to a line at angle α, as illustrated in Figure 3. The plane and the line intersect at a point, which has the radial distance μ from the origin. Varying μ results in a vector of integral values, $I_a(\mu)$ in 2D and $I_{a,\beta}(\mu)$ in 3D:

$$I_a\left(m\right) = \iint f\left(x,y\right)d\left(x\cos a + y\sin a - m\right)dxdy \tag{4}$$

where δ is the Dirac delta function. The simplest surfacelet is the ridgelet transform

$$\Psi_{a,b,a,b} = \left\langle I_{a,b}\left(m\right), y_{a,b}\left(m\right)\right\rangle \tag{5}$$

In general, our generic surfacelet transform is the 1D wavelet transform of the surface integrals.
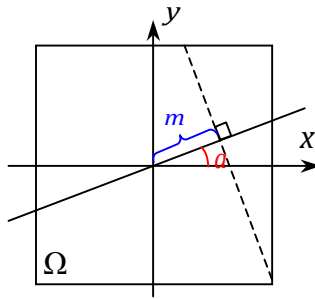
Figure 3 geometric interpretations of parameters in surfacelet transform

Microstructure feature extraction is possible from the results of a Radon transform. Bright spots in the Radon transform image represent line or edge angle and location. Microstructure features can be found computationally from surfacelet representations with parameter values for the features, such as position, orientation, and size. The challenge is that features, such as a fiber or grain boundary, will be represented by several of these bright points close to one another in the Radon transformed parameter space. That only gives us location of a geometry feature but not its size. Therefore, a segmentation step, which gives accurate size of geometry, needs to be integrated into surfacelet transform. Figure 4 shows the process of discovering geometry feature using surfacelet transform. Figure 4a represents an image of 3D voxel dataset of microstructure. The first step of this process is shown in Figure 4b, where the Radon transform is utilized to encode straight-line microstructure feature as points. The output of this step is a matrix of Radon coefficients. In the next step, the peaks in the Radon coefficient matrix are identified and interpreted as indicating grain boundaries. These are shown as colored lines in Figure 4c. The third step, which is shown in the Figure 4d, constructs grains from the grain boundaries. In the final step, the finite element model is constructed by meshing the grains and assigning mechanical properties. Figure 4e briefly shows the FEM analysis result for deformation of the microstructure.
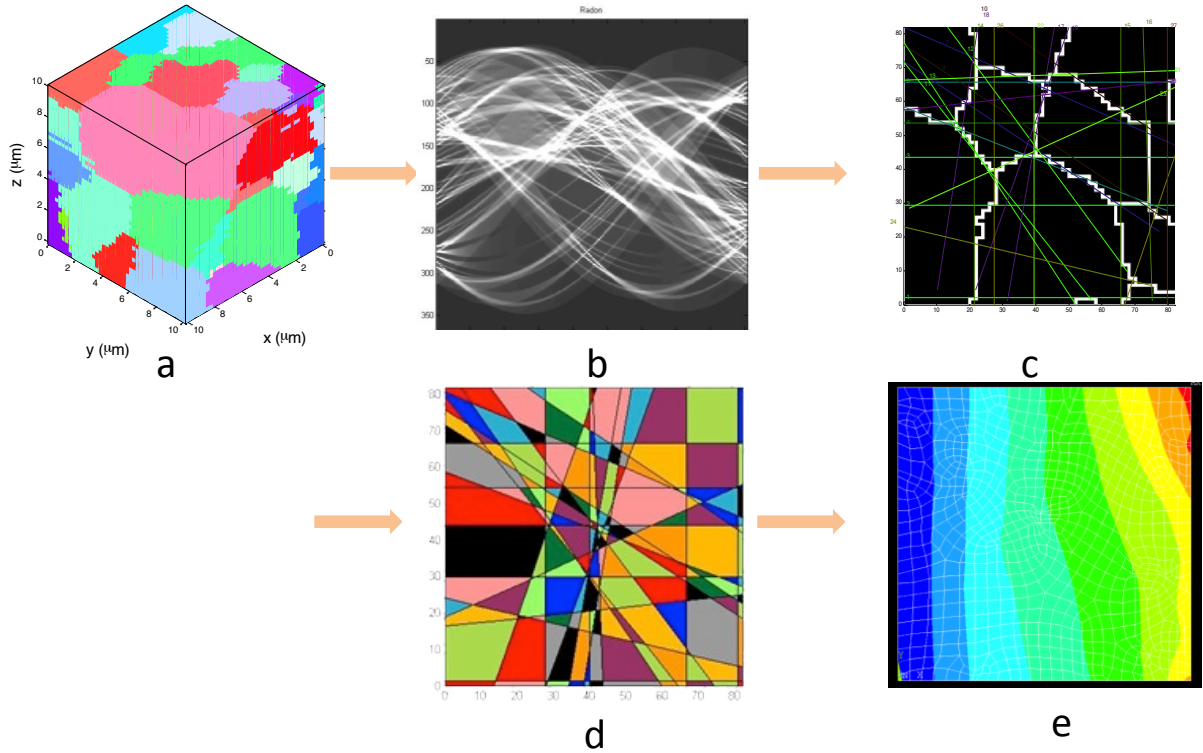
Figure 4 The process of discovering structure-property relationship for metal alloy microstructure a) 3D voxel dataset of microstructure, b) 2D microstructure image, c) Result of the Radon transform of microstructure, d) Result of tentative grain boundaries, and e) FEM analysis result with meshed grain boundaries

3.4   2-point Correlation

N-point correlations provide a rigorous statistical framework to define the spatial correlations of local states in the microstructure [11]. Local state means that any specific location in the microstructure is mathematically defined at the length scale of interest by averaging the information over all the length scales below the selected length scale. Since distributions on local state spaces reflect the probability density associated with finding a specific local state of interest, h, at a point selected randomly in the microstructure, they often are termed the 1-point statistics. 2-point correlations are expanded version of the basic concept that capture the probability density associated with finding local states h and h' at each end of finite-length vectors thrown randomly into a microstructure image. These correlations are only exactly defined over an ensemble of microstructure realizations, but can be approximated if the ability to process many material samples is limited. These n-point correlation methods seek to represent microstructures probabilistically, rather than supporting direct microstructure feature extraction. As such, they represent a basis of comparison for our work, but do not support direct feature extraction and will be not be considered further.

4   RESULTS AND DISCUSSION

In this section, several different microstructure images made by additive manufacturing will be applied to different image processing methods and the result will be shown and described.
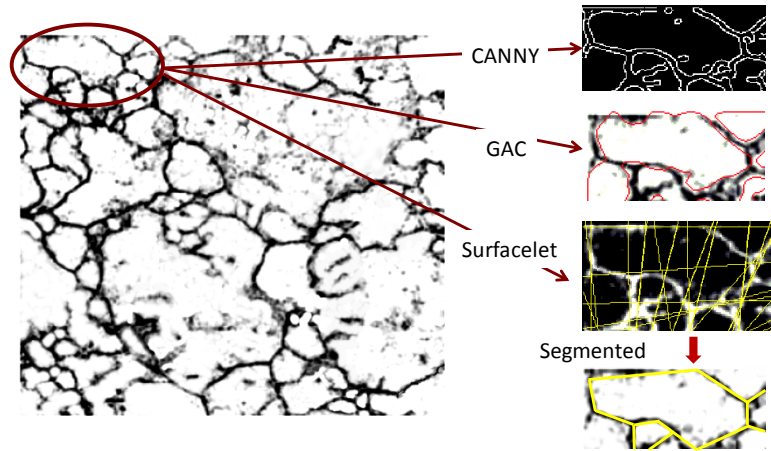
Figure 5 Image processing result of forged part (DIN St45)

A cross sectional microstructure of the forged (DIN St45) part is shown in Figure 5 [12], which will be the sample image used for this example. Forged grain boundaries are of interest in order to quantify grain sizes and shapes. Figure 5 shows the comparison of the three image-processing methods. Geodesic active contour detects a complete grain in red circle area while edge detection can result in incomplete grain boundaries. Since grain boundaries are sometimes discontinuous in the image, edge detection method does not guarantee to produce a closed loop so it fails to extract a grain surrounded by unclear grain boundaries. In contrast, the geodesic active contour model is sensitive to the starting seed location in order to expand properly. Since the surfacelet method does not directly provide length information, the result rarely looks like detected grain boundaries. Lines correspond to grain boundaries in the microstructure image. After length information is integrated into the method, it will detect a grain surrounded by even unclear grain boundaries.
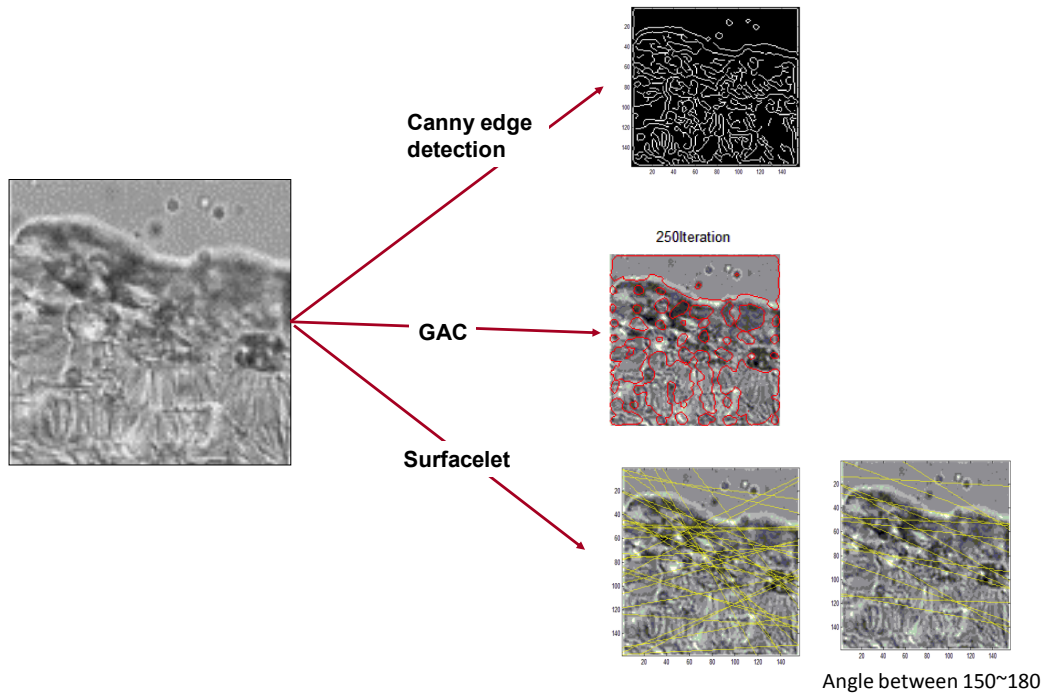
Figure 6 Image processing result of laser sintered nylon-12

Laser sintered nylon-12 is used for another example [13], as shown in Figure 6. Edge detection method works well to find boundaries between un-melted particles and fully melted particles. However, other than edge detection method, geodesic active contour model and surfacelet model does not figure out geometry features in the microstructure image. Un-melted parts of the sample image have a number of fiber-shape or particles. Small image gradients between these microstructure features, which were intended to be detected, prevent them from being recognized.
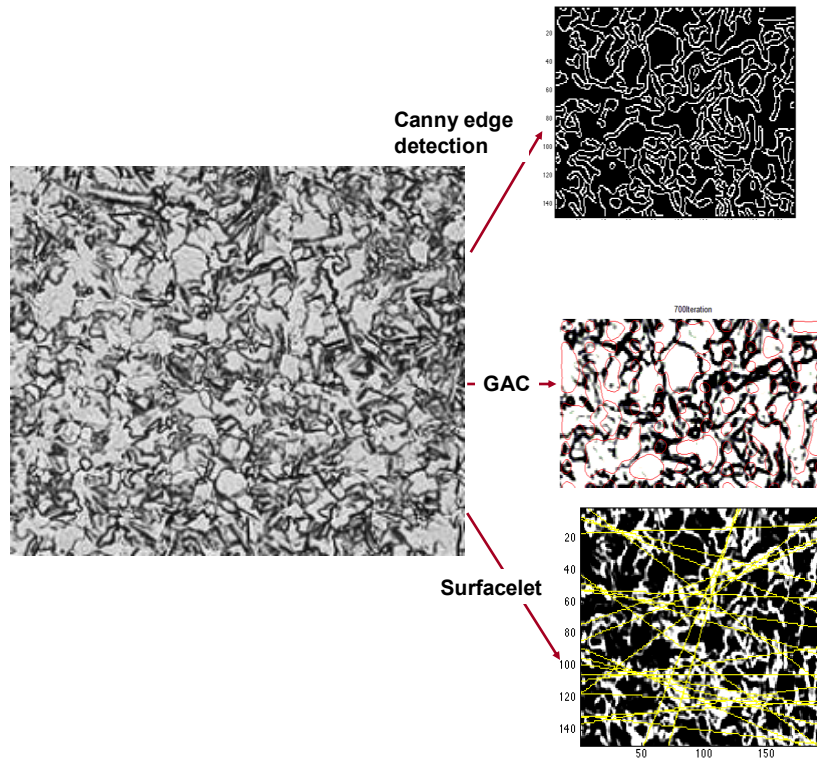
Figure 7 Image processing result of EOS DMLS Titanium

The next example is a metal EOS DMLS Titanium microstructure shown in Figure 7 [14]. The edge detection method extracts all grain boundaries, while the geodesic active contour model detects only parts of grain boundaries. Geodesic active contour only gives good correspondence between contours and grain boundaries when seed contours are located entirely within grains. Hence, seed contours must be positioned and sized so that they are appropriate for the microstructure image. In addition, the gradient of the image gives distinct grain boundaries and affects the good result of geodesic active contour model. In other cases, it provides random results. Results of the surfacelet method show that this method was not effective in recognizing grain boundaries. This is a case where grains are too small and their boundaries are too complex geometrically for the Radon transform to be effective.

683
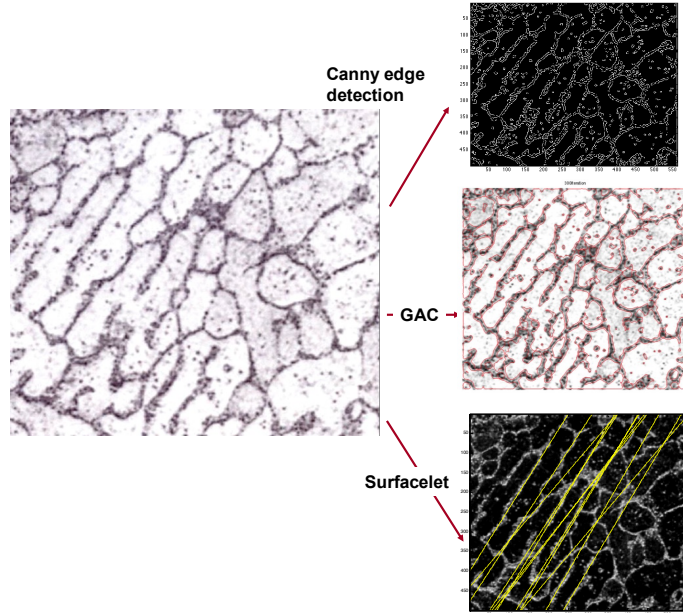
Figure 8 Image processing result of EBM copper

Figure 8 shows an expanded horizontal surface view (normal to the EBM build direction) for EBM fabricated Cu specimen [15]. The example image clearly shows oblong grains with boundaries that are approximately 60-70 degrees from horizontal. The surfacelet method finds them well. Figure 8 only indicates a result of surfacelet in certain range of angle to show the good correspondence between yellow lines and the bright grain boundaries. In addition, edge detection method and geodesic active contour model work well for this example. This is because the sample image includes large contrast between grain boundaries and grain materials.
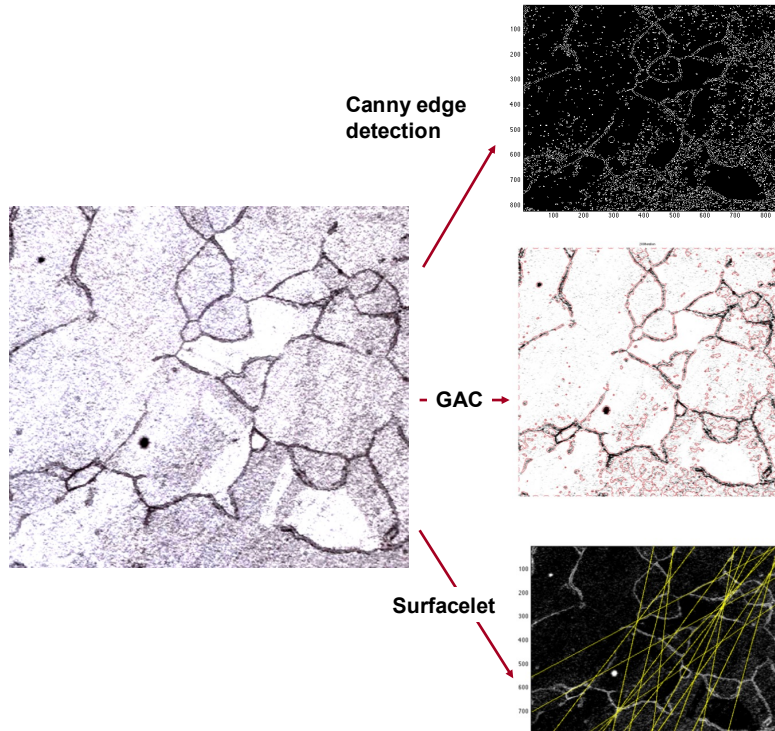
Figure 9 Image processing result of EBM Cobalt-Chrome grains

A cross section of equiaxed grain (including coherent twin grains) in annealed Co-26Cr-6Mo-0.2C fabricated by EBM is shown in Figure 9 [15]. Geodesic active contour finds grain boundaries well until seeds reach un-melted particles in bottom right side of the image. This is because un-melted metal particles give small gradients in the image. The surfacelet method shows good correspondence result between yellow line and bright grain boundaries. However, edge detection method does not give result in finding grains. Noise in the images is detected, although these boundaries are not meaningful. Increased contrast or other image manipulations may lead to improved results.
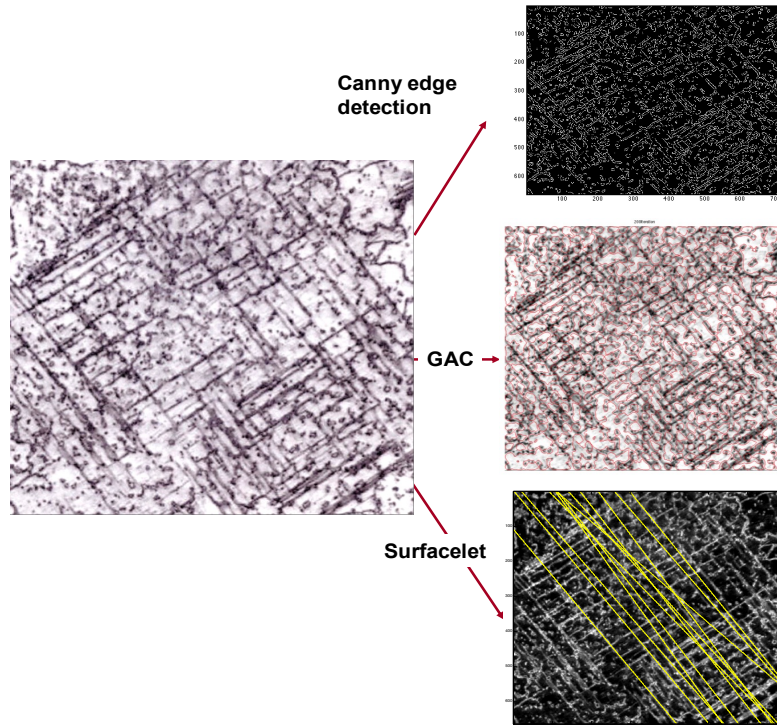
Figure 10 Image processing result of EBM Cobalt Chrome twins

The last example, Figure 10, is an optical microscope horizontal plane image expansion for a Co-base alloy component illustrating twin-fault features at 90° for (100) surface orientation fabricated by EBM [15]. The cross section of this material shows strong orientations to diagonal directions. Since the example image includes these characteristics, the surfacelet method works very well. However, the complexity of the microstructure image and small gradient of the image affect the results of the other image processing methods. Since grains are unclear and microstructure features are not continuous loops, edge detection method detects geometry feature as discrete objects not as grain boundaries and the contour method is ineffective in following boundaries.

Geometry features in microstructure images were extracted by three different image processing methods. Gradients in the image, continuous geometry features, and linearity of the geometry objects are the major influence on the results. Since image processing methods are based on the image gradient, an image with large gradients has better results than smaller gradient. As expected, edge detection methods work well when microstructure features are prominent with large gradients. However, their results are simply binary images with no extracted geometric information about the features. The geodesic contour method worked in cases where microstructure images had well defined grains with closed boundaries. The surfacelet method is designed to extract linear features from images, so the method worked well when grain boundaries were well defined and close to linear in shape.

5   CONCLUSION
In conclusion, in this paper, several image processing methods have been applied to microstructure images to detect geometry features. Several factors such as gradient of image, linearity, or orientation affect the result of the image processing methods. The edge detection method works for finding differences in gradients across the image. However, it finds only

differences in gradients. In order to extract microstructure features as geometric entities and parameters, such as the location of the grain, size, shape, it needs to have an extra step. The geodesic active contour method performs well to find grain boundaries when those boundaries are visually apparent. Since the geometric model is implicit 2-D model, some additional work is needed in order to extract explicit geometric entities. The surfacelet method works well in terms of finding geometric features in the images, provided that segments of the grain boundaries are close to linear and are not too complex. However, it still needs an automation step to construct a complete geometric model of grain boundaries.

REFERENCES

1. Rosen, D.W., N. Jeong, and Y. Wang, *A Hierarchical, Heterogeneous Material CAD Model with Application to Laser Sintering*, in *Solid Freeform Fabrication Symposium*. 2010: Austin TX. p. 619-633.
2. Jain, A.K., *Fundamentals of digital image processing*. 1989: Prentice-Hall, Inc.
3. Bao, P., L. Zhang, and X. Wu, *Canny edge detection enhancement by scale multiplication*. Pattern Analysis and Machine Intelligence, IEEE Transactions on, 2005. **27**(9): p. 1485-1490.
4. Leymarie, F. and M.D. Levine, *Tracking deformable objects in the plane using an active contour model*. Pattern Analysis and Machine Intelligence, IEEE Transactions on, 1993. **15**(6): p. 617-634.
5. Wang, Y. and D.W. Rosen, *Multiscale Heterogeneous Modeling with Surfacelets*. Computer-Aided Design & Applications, 2010. **7**(5): p. 759-776.
6. Canny, J., *A computational approach to edge detection*. Pattern Analysis and Machine Intelligence, IEEE Transactions on, 1986(6): p. 679-698.
7. Kass, M., A. Witkin, and D. Terzopoulos, *Snakes: Active contour models*. International journal of computer vision, 1988. **1**(4): p. 321-331.
8. Caselles, V., R. Kimmel, and G. Sapiro, *Geodesic active contours*. International journal of computer vision, 1997. **22**(1): p. 61-79.
9. Appia, V. and A. Yezzi, *Active geodesics: Region-based active contour segmentation with a global edge-based constraint*, in *2011 IEEE INternational Conference on Computer Vision*. 2011, IEEE. p. 1975-1980.
10. Slaney, M. and A. Kak, *Principles of computerized tomographic imaging*. SIAM, Philadelphia, 1988.
11. Kalidindi, S.R., S.R. Niezgoda, and A.A. Salem, *Microstructure informatics using higher-order statistics and efficient data-mining protocols*. JOM Journal of the Minerals, Metals and Materials Society, 2011. **63**(4): p. 34-41.
12. Bontcheva, N. and G. Petzov, *Microstructure evolution during metal forming processes*. Computational materials science, 2003. **28**(3): p. 563-573.
13. Zarringhalam, H., N. Hopkinson, N. Kamperman, and J. de Vlieger, *Effects of processing on microstructure and properties of SLS Nylon 12*. Materials Science and Engineering: A, 2006. **435**: p. 172-180.
14. Nastase-Dan, C. and S. Comsa, *New Considerations Regarding the Use of Selective Laser Sintering Technology for Biomedical Metalic Implants*, in *1st International Conference on Innovations, Recent Trends and Challenges in Mechatronics, Mechanical*

Engineering and New High-Tech Products Development. 2009: Bucharest, Romania. p. 67-81.

15. Murr, L.E., S.M. Gaytan, D.A. Ramirez, E. Martinez, J.L. Martinez, D.H. Hernandez, B.I. Machado, F. Medina, and R.B. Wicker, *Microstructure architecture development in metals and alloys by additive manufacturing using electron beam melting*, in *2010 Solid Freeform Fabrication Symposium*. 2010: Austin, TX, USA. p. 308-323.